Environ. Sci. Technol. **2005**, *39,* 7678−7683

Advances in Seeded Ambient Temperature Ferrite Formation for Treatment of Acid Mine Drainage

B. E. MORGAN,*,†,‡ O. LAHAV,§ AND R. E. LOEWENTHAL†

Department of Civil Engineering, University of Cape Town, Rondebosch 7701, South Africa, Faculty of Civil and Environmental Engineering, Technion, Haifa 32000, Israel, and Department of Human Biology (Biomedical Engineering), Faculty of Health Sciences, University of Cape Town, Observatory 7925, South Africa

Advances in the seeded ambient temperature ferrite process for treatment of acid mine drainage (AMD) are described. Magnetite formation requires that the oxidation rate of ferrous to ferric does not exceed the rate at which ferrous iron is incorporated into the crystal structure (dehydroxylation−crystallization). If the oxidation rate is too high, then ferric-only oxides form, an effect exacerbated by the presence of calcium. NaOH was used to raise the pH of simulated AMD, which also contained calcium so as to simulate the use of lime (i.e., the dissolved Ca/Fe^{2+} concentration was maintained at 1:1 by the coaddition of $CaCl_2$ because this is the Ca/Fe ratio that occurs when pH is elevated by the dissolution of lime). Raising the pH to 10.5 causes Fe^{2+} to precipitate as "ferrous intermediate" (FI), which is then partially oxidized to magnetite (Fe^{2+}-$Fe^{3+}{}_2O_4$). The inhibitory effect of calcium is overcome by a combination of magnetite seed particles, high FI concentrations, and aging. High FI concentrations are easily obtained, even from AMD low in Fe^{2+}, by a contact stabilization reactor−settler sequence. Results for simultaneous removal of cobalt, a metal found in significant concentrations in South African AMD, are also presented.

Introduction

Acid mine drainage (AMD) is characterized by low pH, variable iron concentrations, significantly high concentrations of nonferrous (mainly heavy) metals, and very high salinity, principally in the form of sulfate (*1*, *2*). The ambient temperature ferrite process (ATFP) approach to metal removal from AMD is centered on the iron oxide magnetite ($Fe^{2+}Fe^{3+}{}_2O_4$) (*3*−*5*). Magnetite has several key properties that make it an ideal end product of oxidation for metal removal from AMD: It has excellent settling properties and forms a high-density, rapidly dewatering sludge that is very stable at low pH values, and moreover, it has the capacity to affect nonferrous metal removal and stabilization via cation substitution. Furthermore, magnetite is a commodity of significant commercial value.

The formation of magnetite, which is comprised by both ferrous and ferric ions, from oxidation of ferrous solutions requires the oxidation rate of ferrous to ferric to not exceed the rate at which ferrous iron can be stabilized within the crystal structure. The rate-limiting step during crystallization is the transformation of freshly formed "hydrated magnetite" into crystallized magnetite through a dehydroxylation (or dehydration) reaction (*7*). If the rate of oxidation of ferrous species exceeds the rate of dehydration−crystallization, then the formation of ferric-only oxyhydroxide end products (e.g., FeOOH) becomes significant (*5*, *7*−*9*). In the ATFP described here, such "overoxidation" is avoided by (1) the presence of a high magnetite seed concentration (*4*, *5*, *9*), (2) a novel means of maintaining a steady-state threshold "ferrous intermediate" (FI) concentration, (3) a controlled oxidation rate, and (4) an aging period during which freshly formed magnetite is left to settle without mixing or aeration, allowing time for dehydration−crystallization to occur.

The ATFP can be operated as either a one-step process in which ferrous oxidation and ferrite precipitation occur together (*4*, *5*, *11*) or a two-step process where two-thirds of the AMD is first oxidized (to Fe^{3+}) and then recombined with the other one-third (Fe^{2+}) in a precipitation step (*12*, *13*). The ATFP has been successfully applied to industrial wastewaters containing dissolved metals. In these cases, NaOH is usually used to elevate the pH (*14*). The difficulties facing the application of the conventional ATFP to AMD are the massive dissolved metal loads involved and the accordingly stoichiometrically determined pH-elevating agent molar requirements that render the costs of NaOH prohibitive. Although lime is an economical agent for raising pH, calcium is well-known to inhibit ferrite formation (*3*, *11*, *12*). The mechanism of calcium interference is not understood (*17*), but Choung et al. (*21*) provide the most pertinent clue: Lime or NaOH were used to raise the pH of separate ferric and ferrous solutions that were then combined, allowing ferrites to form. Calcium interference occurred with lime + ferric rather than lime + ferrous combinations, suggesting involvement of a hydrated calcium−ferric complex.

Nevertheless, Perales Perez et al. (*11*) and McKinnon et al. (*3*) demonstrated in a one-step and two-step fashion, respectively, how magnetite seed could be used to overcome the inhibitory effect of calcium in ambient temperature ferrite formation. Working with one-step batch experiments, Lahav et al. (*5*) further developed the use of seed by delineating boundary conditions with respect to oxidation rate, seed concentration, pH, and temperature within which magnetite is attained as the predominant end product of oxidation of ferrous solutions. With respect to temperature, the process was found to function at temperatures as low as 7 °C (*5*). Morgan et al. (*10*) investigated the conditions required for optimal seeded-ferrite formation from ferrous solutions under steady-state one-step conditions, both in the absence and presence of calcium. Notably, a threshold concentration of metastable, amorphous solid "ferrous intermediate" species (as distinct from stable, crystallized ferrous−ferric or ferric-only end products) below which pure magnetite does not form was shown to exist. In the absence of Ca^{2+} and with a magnetite seed concentration of ∼20 g Fe/L, pure magnetite could be formed only when the FI concentration in the oxidation reactor was maintained above ∼500 mg Fe/L. Using magnetite seed in the presence of calcium, Morgan et al. (*10*) found that the FI concentration must be elevated to at least ∼1700 mg Fe/L to attain pure magnetite.

In this paper, the role of aging in seeded ambient temperature ferrite formation in the presence of calcium is examined. In addition, proof-of-concept results for heavy metals removal by seeded ambient temperature ferrite

* Corresponding author phone: 27-21-4066840, fax: 27-21-4487226; e-mail: bmorgan@cormack.uct.ac.za.
† Department of Civil Engineering, University of Cape Town.
‡ Department of Human Biology, University of Cape Town.
§ Technion.

10.1021/es050498a CCC: $30.25

Published on Web 08/25/2005

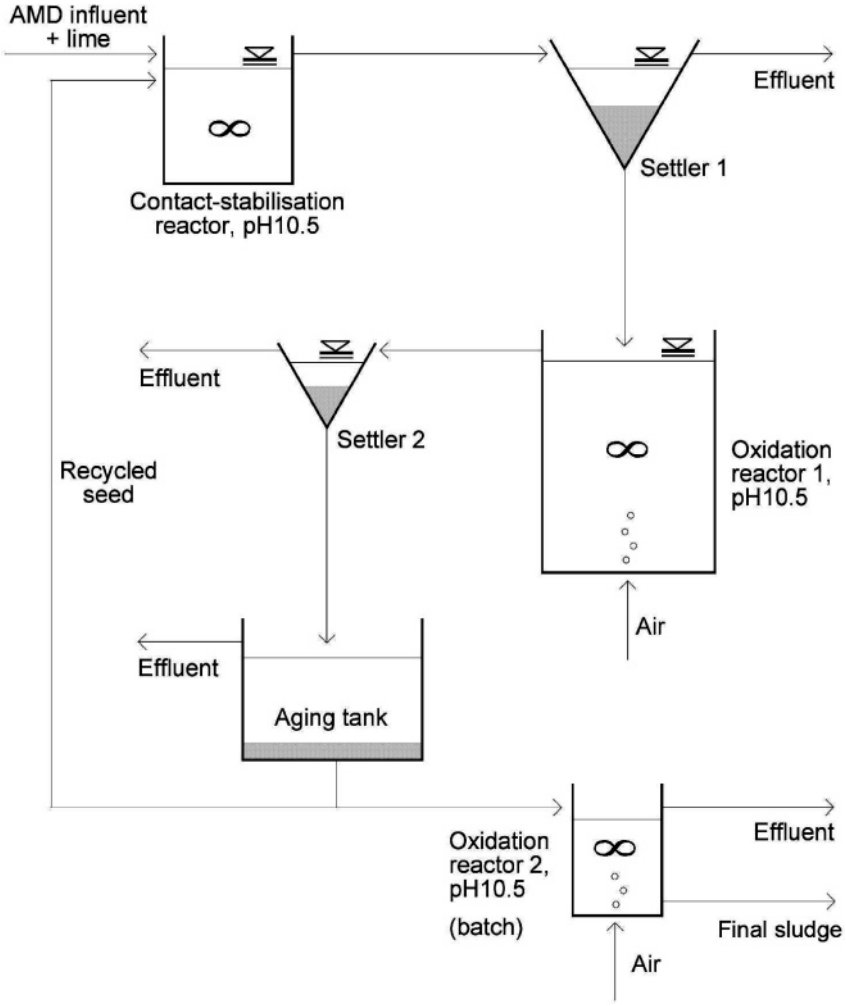

FIGURE 1. Schematic representation of the seeded ambient temperature ferrite process.

TABLE 1. Typical Ranges (mg/L) of Ferrous Iron and the Four Transition Metals Found in Next Highest Concentrations in AMD from a Gold Mine in the Western Witwatersrand Region of South Africa (*15*)

Fe	Mn	Ni	Co	Zn
680−1760	18−43	5−28	2−5	1.4−3.2

formation in the presence of calcium for the case of cobalt (Co/Fe = 1:10) are presented. Cobalt is the transition metal found in highest concentration after Mn and Ni in AMD typical of the Westrand mining region of South Africa (*2*) (Table 1). Co was chosen because it is more readily incorporated into magnetite under ambient temperature conditions than Ni (*16*) and Mn presents particular pH-dependent precipitation problems (see ref *3*, for example), which are the subject of separate research.

Experimental Section

Process Description. The continuously operated process is depicted in Figure 1. Simulated AMD (hereafter referred to as AMD) was combined with a suspension of magnetite seed composed of cuboidal particles ~0.1 μm in dimension (*4*) at a concentration of 15−20 g Fe/L in a contact stabilization reactor. Here, the mixture is maintained at pH 10.5 by the constant addition of 1.5 M NaOH without any active aeration apart from that caused by mixing. In this reactor, Fe^{2+} in the AMD precipitates to form FI, which instantly and completely adsorbs to the magnetite seed as inferred from settling behavior, which rapidly yields a clarified supernatant with <1 mg Fe/L. If seed is not present, then FI forms voluminous flocs that take a long time to settle. The retention time in the contact stabilization reactor therefore need be only a few seconds but in practice was ~15 min. The mix consisting of seed and adsorbed FI then flows to a gravitational settler where the magnetite seed and all precipitated components adsorbed to it are concentrated. The bulk AMD water volume (~65% of original flow) is drawn off, and the concentrated seed and precipitated components adsorbed to it are pumped to the first oxidation reactor. Here, air is injected from below through a porous stone diffuser, and the newly precipitated FI is partially oxidized to become fresh *hydrated* ferrites. The air flow rate is limited so as to maintain the FI concentration at a suprathreshold steady state as discussed above. The retention time in the first oxidation reactor is around 6 h (Table 3). The mixed contents of the oxidation reactor then flow into a second settler where the bulk (~95%) of the water is drawn off. The remaining solids comprising original ferrite seed, fresh hydrated ferrites, and FI are then transferred with their mother liquor to an aging tank for a given amount of time. The aging tank was neither aerated nor mixed. To maintain the seed concentration in the first oxidizing reactor at 15−20 g Fe/L, a fraction of aged solids in their liquor was constantly recycled to the contact stabilization reactor. The remaining aged solids in their liquor were transferred to a second oxidation reactor where all remaining FI was further partially oxidized to the point of being exhaustively trans-

TABLE 2. Effect of Aging Period on the Percentage Ferrous in the Final Precipitate[a]

aging period (h)	% Fe^{2+} in precipitate (%)
18	30.1
6	28.0
3	28.1
2	< 25

[a] FI concentration ≈2 g Fe/L; recycled magnetite seed concentration = 15−20 g Fe/L.

TABLE 3. Effect of Oxidation Rate on the Percentage Ferrous in the Final Precipitate[a]

volume of oxidation reactor (L)	retention time (h)	aging (h)	oxidation rate (mg Fe/(L/min))	% ferrous in precipitate
5.2	6.1	3	8.30	28.1
5.2	6.1	6	8.31	28.0
2	2.22	6	23.22	22.6
1.2	1.33	6	40.15	19.7

[a] FI concentration ≈ 2 g Fe/L; seed = 15−20 g Fe/L.

formed into fresh hydrated ferrite prior to final aging and disposal.

Establishment of the suprathreshold FI concentration in the first oxidation reactor is independent of the Fe^{2+} concentration in the raw AMD because the FI concentration in the first oxidation reactor can be built up to any level so desired by withholding oxidation (aeration). When oxidation is withheld, the FI concentration adsorbed to the seed increases with each cycle. (Even though FI is a solid mass rather than a dissolved concentration, the term concentration is used because FI is measured at pH 2 where it becomes Fe^{2+} in solution.) When the desired FI concentration is attained, aeration (oxidation) of the first oxidation reactor is commenced at a rate adjusted to be equal to the rate required to transform into ferrite only new ferrous entering the system; i.e., a steady-state FI concentration is maintained. The time to reach a certain steady-state FI concentration prior to the onset of oxidation is short (e.g., 10 h for a target steady-state FI concentration of 2000 mg Fe/L) and is independent of both the concentration of ferrous in the raw AMD and the flow rate of the raw AMD.

In the experiments reported in this paper, only NaOH was used to raise pH, the use of lime being simulated by the addition of calcium as described in the text: contact stabilization reactor = 2.5 L, first settler = 5 L (allowing >5 times theoretical RT), first oxidation reactor = 5.2 L (based on an anticipated oxidation rate of ∼10 mg Fe/(L/min)), second settler = 2.5 L (allowing >5 times theoretical RT), second oxidation reactor = 2.5 L (operated batch style, see ref *5*). A 20-L bucket was used as an aging tank. At the end of each aging period, the supernatant was manually poured off and the remaining seed and liquor was mixed by hand and transferred to a continuously mixed compartment (not shown) from where it was automatically pumped into the contact stabilization reactor at a rate adjusted so as to maintain the seed concentration in the oxidation reactor at 15−20 g Fe/L.

Experimental Procedure and Analysis: All reagents were acquired from Kimix, Cape Town, South Africa, and were of analytical grade. A solution of 0.359 M ferrous sulfate and 0.359 M sodium sulfate ($Fe^{2+}/SO_4^{2-}/Na^{2+}$ = 1:2:2 to resemble AMD), brought to 2.7 < pH < 3 by the addition of 2 mL/L of 32% HCl (to avoid oxidation by atmospheric oxygen) served to simulate AMD. The experiments were conducted in a way that simulates the use of lime ($Ca(OH)_2$), and only 1.5 M NaOH was used to raise the pH. Lime was simulated by adding an aqueous 0.359 M calcium chloride solution in parallel with the simulated AMD so that the moles of Ca equal the moles of Fe according to the stoichiometry of

$$Ca(OH)_2 \rightarrow Ca^{2+} + 2OH^-$$

$$Fe^{2+} + 2OH^- \rightarrow Fe(OH)_2$$

Under these conditions, calcium is saturated with respect to calcium sulfate as demonstrated by the rapid appearance of gypsum particles in the contact stabilization reactor and first settler. These gypsum particles did not reach the oxidation reactor in significant amounts (i.e., no buildup on the walls of the first oxidation reactor as was seen in the contact stabilization reactor and first settler). Calcium reaching the first oxidizing reactor is therefore largely dissolved calcium whose concentration is governed by the solubility of gypsum. Theoretical calculations including Debye−Hückel effects predicted a dissolved calcium concentration of 287.5 mg/L, which accorded well with empirical measurements (data not shown).

Magnetite used for the initial start-up seed was made under ambient temperature conditions previously described (*5*). AMD (in parallel with calcium chloride as described above) was continuously pumped into the contact stabilization reactor at a constant load of 15 mL/min (60 mg Fe/min). In all experiments, both reactors were mixed at 200 rpm and completely mixed conditions were attained. In the experiments investigating the effect of oxidation rate, the volume of the first oxidizing reactor was varied. In all experiments, air was introduced from below into the first oxidizing reactor at an airflow rate sufficient to keep the FI concentration in the first oxidation reactor at a suprathreshold concentration (*10*) of ∼2000 mg Fe/L. The pH was maintained at 10.5 (*5*, *10*) in the contact stabilization and oxidation reactors by the automatic addition of a 1.5 M NaOH solution, and the temperature was maintained at 22 ± 2 °C. Dissolved oxygen (DO) concentration was continuously measured in the second oxidation reactor using a YSI 55 DO meter. Oxygen in the second oxidation reactor was also introduced by the injection of air, and oxidation was considered complete when the DO rose from ∼0 to >8 mg/L. (See Figure 3 in ref *4*.)

Solid leachability was assayed in synthetic acid rain, which simulates many years of natural exposure (*6*). A sample of sludge was aged for 3 weeks and then filtered at pH 2 to remove any residual FI. The solids remaining on the filter were then dried at room temperature, weighed, and submerged in 1 L of synthetic acid rain consisting of sulfuric acid/nitric acid in a 1:1 molar ratio, diluted to pH 5 with distilled water. pH was monitored, and 1-mL samples of the leachate were taken and measured for Fe.

pH, FI (phenanthroline method), total iron, and calcium (atomic absorption) concentrations were measured in each reactor compartment at various times. In this study, the term "total iron" (Fe_T) represents the iron in a 1-mL sample of mixed liquor from the oxidation reactor, which undergoes complete dissolution in 32% HCl within 15 min. This includes magnetite seed and/or other end products of oxidation but not FI because the 1-mL sample was diluted in 100 mL of 0.01 M HCl (i.e., pH 2) before being filtered: End products remain on the filter (0.45 μm), but FI dissolves and leaves with the filtrate. End products were then dissolved in 32% HCl before being diluted to a concentration and pH suitable for total iron and ferrous measurements. The Fe^{2+}/Fe_T concentration ratio expressed as percentage ferrous content of the end product was determined from these results. Structural characterization of the dried sludge was performed by using X-ray diffractometry (XRD) using a Phillips PW3710 XR diffractometer with a copper target (Kα radiation). Effluent from the first settler only was analyzed, and fine particles

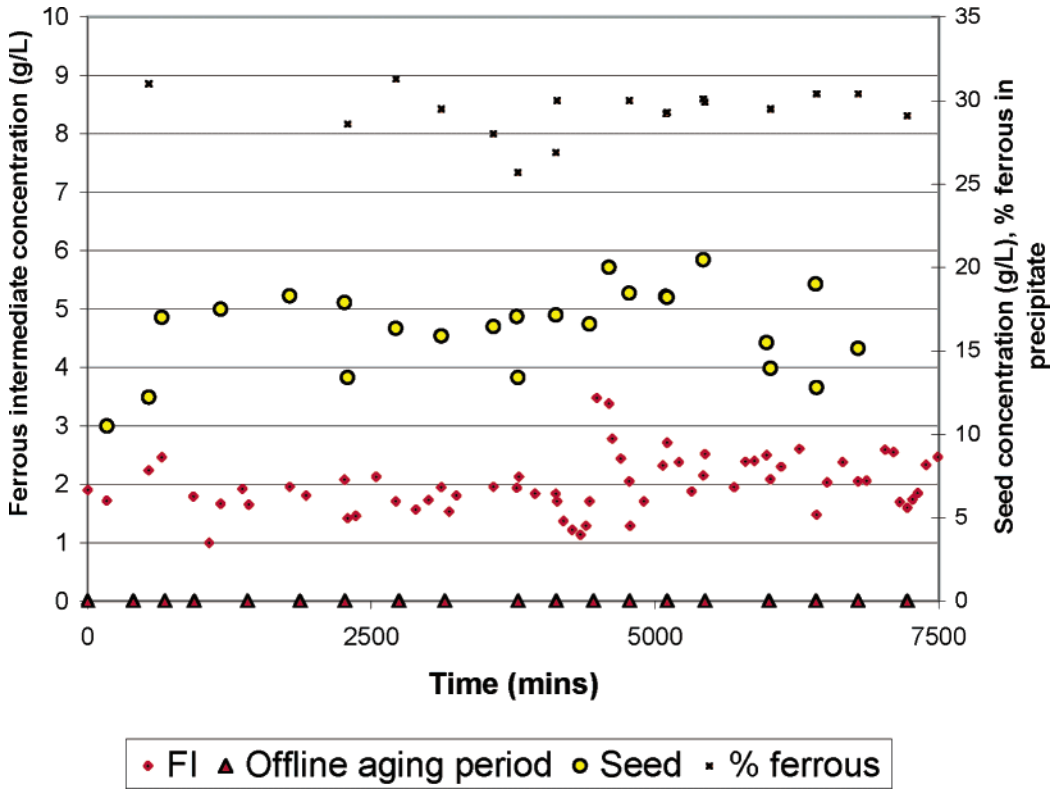

FIGURE 2. Steady-state data for an experiment performed in the presence of calcium with a ferrous intermediate (FI) concentration of 2 ± 0.48 g Fe/L and an aging period of 17.31 ± 1.67 h.

("fines") suspended in the effluent were quantified according to the method previously described (*5*) whereby 100 mL of supernatant taken from a depth of 30 mm below the surface of the effluent in the first settler were filtered (0.45 μm). The filtered fines were dissolved in HCl and measured for Fe expressed in mg/L. The filtrate was similarly measured.

SVI (volume occupied by 1 g Fe of sludge after a settling time of 30 min) was determined by transferring 1 L of mixed reactor contents to a 1-L measuring cylinder (*22*). Prior to settling, the mixture was well-mixed, and a 1-mL sample was taken to determine Fe concentration.

Results and Discussion

Aging Time and Oxidation Rate. In the presence of calcium (Fe/Ca = 1:1), simulating the use of lime, Morgan et al. (*10*) reported that a steady-state FI concentration of ~1700 mg Fe/L resulted in substantially pure magnetite with a 30% ferrous fraction without mentioning any need for aging. More recent attempts to repeat the latter result were unsuccessful, resulting in magnetite of ~26% ferrous and the formation of significant concentrations of ferric-only end products (data not shown). It is here reported that as a result of insufficient automatic control equipment an overnight aging period of ~18 h had in fact been allowed between oxidation periods of ~6 h in the original experiments reported by Morgan et al. (*10*). Figure 2 presents data for a repeat experiment in which an explicit "off-line" aging period of ~18 h was introduced. In the repeat experiment, magnetite formation with a ferrous fraction of ~30% was again found to be the sole end product of oxidation.

The time along the *x*-axis represents the accumulated oxidation period in minutes. Each "off-line" aging period (meaning that continuous operation was not interrupted during aging) is marked along the *x*-axis with a small triangle. Total duration of oxidation was for 4.26 seed ages where a seed age equals the time required to reproduce the initial seed mass present in total in all reactor compartments at the beginning of the experiment.

Reducing the aging period from 18 to 3 h resulted in a small reduction in the percentage ferrous in the steady-state end product (Table 2). (With respect to the end product, steady-state was defined as no significant variation in percentage ferrous among three measurements taken at least 3 h apart after more than three seed ages had elapsed.) Below an aging period of 3 h, the percentage ferrous value rapidly decreased to 25% before steady state had been reached. Under the experimental conditions used here, a minimum aging period of 3 h is therefore required to produce magnetite with a ferrous fraction of greater than 28%.

Since successful magnetite formation depends on the balance between rate of oxidation and the time allowed for dehydration−crystallization (aging period), these two parameters were investigated in relation to one another (Table 3). Taking the data in row 2 of Table 3, where the percentage ferrous in the end product was 28.0%, as an example, the oxidation rate in this case is 1.0−0.28 = 0.72 of the ferrous disappearance rate. At steady-state, AMD was introduced and disappeared at 60 mg Fe^{2+}/min giving an oxidation rate of 0.72 × 60 = 43.2 mg Fe^{2+}/min or 8.3 mg Fe^{2+}/(L/min) (divide by 5.2 L, the volume of the oxidation reactor). Rows 2 and 3 in Table 3 show that as the volume of the oxidation reactor was reduced, resulting in a shorter retention time (RT), the oxidation rate needed to be increased to maintain the FI concentration in the oxidation reactor at steady state. The effect of the higher oxidation rate was a decrease in the percentage ferrous in the fresh precipitate. The data points given in Table 3 suggest a linear relationship between the rate of oxidation and the percentage ferrous in the fresh precipitate when calcium was present (R^2 = 0.9663, n = 4). Lahav et al. (*5*) also found a linear relationship between oxidation rate and percentage ferrous for magnetite formation in the absence of calcium. Under the latter conditions the maximal oxidation rate compatible with a percentage ferrous

fraction of 29% was ~14 mg Fe^{2+}/(L/min). In the present experiments performed under similar conditions but in the presence of calcium, the rate of oxidation compatible with a percentage ferrous of 28% was 8.3 mg Fe^{2+}/(L/min) (Table 3, rows 1 and 2). Since these two conditions only differ slightly in seed and FI concentration and, above a certain threshold, neither of the latter two affect the maximal oxidation rate (*5*, *10*), the only other factor that can account for the difference in maximal oxidation rate can be the presence of calcium. The presence of calcium therefore seems to limit the maximum ferrous oxidation rate at which magnetite is formed, relative to the case where calcium is absent by a factor of ~0.6. The longer aging period required when calcium is present indicates that calcium retards the rate of dehydroxylation−crystallization. Since dehydroxylation−crystallization does not only begin once undisturbed aging begins but commences upon the formation of hydrated magnetite *during* active oxidation (*17*), it is to be expected that calcium exerts the same retarding effect on the rate of dehydroxylation−crystallization during oxidation, and hence for ferrite formation to succeed, the oxidation rate must be decreased in proportion to the decreased rate of dehydroxylation−crystallization.

Role of the Contact Stabilization Reactor−Settler Sequence. The pH of the contact stabilization reactor, as for the oxidation reactor, was maintained at 10.5. The dissolved iron present in the raw AMD introduced into the contact stabilization reactor therefore fully precipitates as FI and is immediately adsorbed onto the magnetite seed. The near-instantaneous time required for these steps allows for a relatively small contact stabilization reactor. The effluent from the contact stabilization reactor containing magnetite seed coated with FI then reaches the settler. The seed particles greatly enhance the settling of the FI phase, which would otherwise, in the absence of seed, form a bulky voluminous floc with very poor settling properties (SVI ≈ 100 mL/g Fe). In contrast, the SVI of the contents of the contact stabilization reactor was found to be 30 mL/g Fe, and the separation ratio after 30 min of settling time was 35:100 (solids/total volume). Extending the settling time beyond 30 min did little to diminish the sludge/water ratio.

The contact stabilization reactor−settler sequence therefore increased the concentration of FI in the underflow of the settler ~3 times relative to the concentration of dissolved iron in the raw AMD. This has two important effects. First, dissolved calcium does not concentrate at the bottom of the settler in the way solid FI adsorbed to magnetite seed does. Consequently, the FI/dissolved calcium concentration ratio in the underflow is also elevated by a factor of at least ~3. It is in this way that the enhanced FI/dissolved calcium concentration ratio, essential in overcoming the inhibitory effect of calcium on ferrite formation (*10*), is attained.

Second, the bulk AMD water volume (~65%), now virtually devoid of all metal intermediates (e.g., Table 4, row 3) is drawn off the top of the first settler, and the concentrated seed and precipitated components in the underflow are pumped to the oxidation reactor. The hydraulic retention time of approximately two-thirds of the total AMD flow is thus independent of the rate-limiting step in the ATFP, i.e., the aging step, and is limited only by the very much faster first settling step. Similarly, ~95% of the AMD water reaching the first oxidation reactor is drawn off prior to the next two steps in the sequence, aging and either recycling or exhaustive oxidation. The volume of AMD requiring oxidative treatment is thus rapidly and sequentially diminished, and the volume requiring aging is similarly relatively small: Only ~5% of ~35% of the total AMD volume requires aging, and even less than this amount requires recycling.

Effluent and Sludge Characteristics. Under experimental conditions of FI = ~2 g Fe/L and an aging period of 6 h, the total iron concentration in the effluent leaving the settling tank was always less than 1.0 mg Fe/L, and the final sludge, composed of essentially pure magnetite as determined by XRD (data not shown) and the Fe^{2+}/Fe_T ratio, settled exceptionally well (SVI = 3.2 mL/g Fe). After standing in an open beaker at room temperature for 3 weeks, the wasted sludge dried into a hard cake with an iron content of ~65% and a total solids content of 93%.

TABLE 4. Data for the Influent, Effluent, and Final Precipitate for the Experiment in Which Cobalt and Calcium Were Present[a]

sample	concentration (mg/L)	Co^{2+}/Fe^{2+} molar percentage (%)
influent	$Fe^{2+} = 3909$ $Co^{2+} = 421$	10.60
effluent: dissolved fines	$Fe^{2+} = 6.22$ $Co^{2+} = 0.64$	10.78
effluent: filtrate	$Fe^{2+} < 0.06$ $Co^{2+} = 0.09$	
final precipitate $Fe^{2+}/Fe_T = 32\%$	$Fe^{2+} = 177.6$ $Co^{2+} = 17.23$	9.70

[a] The molar percentage values of the effluent fines and final precipitate reflect the Co^{2+}/Fe^{2+} ratio in the influent, i.e., ~10%.

Stability of the Final Precipitate. After a period of 3 weeks in synthetic acid rain, percentage mass loss from a 60-mg (dry mass) sample of sludge was <0.05% (mg dissolved Fe/mg total Fe) and remained so for up to 10 weeks. There was no significant change in the pH of the leachant during this time.

Ferrite Formation in the Presence of Cobalt and Calcium. A proof-of-concept experiment for nonferrous metal removal was performed using cobalt. Both calcium and cobalt were present in the influent (Ca^{2+}/Fe^{2+} = 1:1, Co^{2+}/Fe^{2+} = 1:10). Co^{2+}/Fe^{2+} = 1:10 far exceeds the ratio of these metals in any South African AMD water, an arbitrarily high ratio being chosen simply to test the process. In this experiment, the seed concentration was maintained at 17.4 ± 2.3 g Fe/L and the FI concentration was 3.2 ± 0.7 g Fe/L. The oxidation rate was 8.5 mg Fe/(L/min). Under these conditions and with an aging period of 6 h, brown ferric-only end products quickly appeared in the oxidation reactor and the percentage ferrous in the fresh end products declined rapidly. Only when the aging period was increased to 24 h did no brown end products appear, and the percentage ferrous in the fresh precipitate remained stable at an average of 32.61 ± 1.25% over eight seed ages. (For this experiment, the starting seed mass was 160 g and one seed age was 53.3 h). Since aging occurs "off-line" and more seed is being generated than is being recycled, aged seed will accumulate. Increasing the aging period to 24 h when Co is present therefore presents no practical problem.

XRD software (*18*) identified this precipitate as the ferrite "cobalt iron oxide" (*19*). Chemical analysis however showed that the Co/Fe ratio in this sample was 9.7:100 (Table 4), whereas the Co/Fe ratio in stoichiometric cobalt iron oxide ($CoFe_2O_4$) is 1:2. The precipitate therefore probably comprises a mixture of magnetite (~90%) and $CoFe_2O_4$ (~10%) although the presence of small amounts of poorly crystalline solids containing cobalt cannot be excluded.

Although the effluent filtrate was essentially free of iron and cobalt (row 3 of Table 4), the concentration of these elements present as "fines" in the effluent was significant. The size of these particles has not been determined, and their removal has not been investigated. The latter may be affected by magnetic separation techniques, longer settling times, or flocculation−coagulation methods.

Nonferrous metals are well-known to interfere with ferrite formation in both the presence and the absence of calcium,

and the degree of interference varies from one metal to another (*3*). The order of interference was found to vary according to whether lime (Cu > Ni ≈ Zn) or NaOH (Zn ≈ Ni > Cu) was used (*3*). Magnetite seed mitigates nonferrous metal interference. The longer aging time required when Co is present is therefore unsurprising although the precise mechanism of interference is not known. That a longer aging time overcomes Co interference suggests that Co retards the rate of dehydroxylation−crystallization relative to oxidation.

Scaleup and Commercial Factors. The process design depicted in Figure 1 presents in our opinion only few scale-up problems. Remobilization of settled aged seed required for recycling will require a suitable mixing mechanism. After an aging period of 24 h or less, seed settles as a thin paste that is readily resuspended. Once suspended, at the seed densities (up to ∼20 g Fe/L) used in these experiments, the viscosity of the suspension is only slightly higher than that of water, and no handling problems, even at flow rates as low as ∼10−15 mL/min, were encountered.

Operational costs can be offset by the commercial value (>$110/ton) of the high-quality (defined as an Fe content >68%) ferrite seed end product (*20*). Major users of magnetite are coal-washing and steel production plants. Furthermore, magnetite's combination of high-density, low scratch visibility, and excellent ecological characteristics have prompted its escalating use as a filler in polymers and rubbers, for example, in the production of automotive sound dampening mats (*20*).

Acknowledgments

The Water Research Commission of South Africa provided financial support without which this work would not have been possible.

Literature Cited

(1) Lambert, D. C.; McDonough, M.; Dzombak, D. A. Longterm changes in quality of discharge water from abandoned underground coal mines in Uniontown Syncline, Fayette County, PA. *Water Res.* **2004**, *38*, 277−288.

(2) Wittmann, G. T. W.; Förster, U. Heavy metal enrichment in mine drainage: II. The Witwatersrand goldfields. *S. Afr. J. Sci.* **1976**, *72*, 365−370.

(3) McKinnon, W.; Choung, J. W.; Xu, Z.; Finch, J. A. Magnetic seed in ambient temperature ferrite process applied to acid mine drainage treatment. *Environ. Sci. Technol.* **2000**, *34*, 2676−2581.

(4) Morgan, B. E.; Loewenthal, R. E.; Lahav, O. Fundamental study of a one-step ambient temperature ferrite process for treatment of acid mine drainage waters. *Water SA* **2001**, *27* (2), 277−282.

(5) Lahav, O.; Morgan, B. E.; Hearne, G.; Loewenthal, R. E. A one-step ambient temperature ferrite process for treatment of acid mine drainage waters. *J. Environ. Eng.* **2003**, *129* (2), 155−161.

(6) Aube, B. C.; Zinck, J. M. Comparison of AMD treatment processes and their impact on sludge characteristics. *Mining and the Environment II, Sudbury '99*, Sudbury, Ontario, Canada, Sept 12−16, 1999.

(7) Cornell, R. M.; Schwertmann, U. *The Iron oxides: Structure, Properties, Reactions, Occurrence and Uses*; VCH: Weinheim, Germany, 1996.

(8) Blesa, M. A.; Matijevic, E. Phase transformations of iron oxides, oxo-hydroxydes, and hydrous oxides in aqueous media. *Adv. Colloid Interface Sci.* **1989**, *29*, 173−221.

(9) Perales Perez, O.; Umetsu, Y. ORP-monitored magnetite formation from aqueous solutions at low temperatures. *Hydrometallurgy* **2000**, *55*, 35−56.

(10) Morgan, B. E.; Lahav, O.; Hearne, G. R.; Loewenthal, R. E. A seeded ambient temperature ferrite process for treatment of AMD waters: Magnetite formation in the presence and absence of calcium ions under steady-state operation. *Water SA* **2003**, *29* (2), 117−124.

(11) Perales Perez, O.; Umetsu, Y.; Sasaki, H. Precipitation and densification of magnetic iron compounds from aqueous solutions at room temperature. *Hydrometallurgy* **1998**, *50*, 223−242.

(12) Wang, W.; Xu, Z.; Finch, J. A. Fundamental study of an ambient temperature ferrite process in the treatment of acid mine drainage. *Environ. Sci. Technol.* **1996**, *30*, 2604−2608.

(13) Tamaura, Y.; Tu, P. Q.; Rojarayanont, S.; Abe, H. Stabilization of hazardous materials into ferrites. *Water Sci. Technol.* **1991**, *23*, 399−404.

(14) Tamaura, Y.; Katsura, T.; Rojarayanont, S.; Yosida, T.; Abe, H. Ferrite process; Heavy metal ions treatment system. *Water Sci. Technol.* **1991**, *23*, 1893−1900.

(15) Data supplied by Randfontein Estate Mine. Private communication, 2000.

(16) Perales Perez, O. University of Puerto Rico, Mayagüez, PR. Private communication.

(17) Perales Perez, O.; Tohji, K.; Umetsu, Y. Theory and practice of the removal of heavy metal ions by their precipitation as ferrite-type compounds from aqueous solution at ambient temperature. *Metall. Rev. SA* **2001**, *17* (2), 137−180.

(18) *Philips X'pert Data Analyzer*; Koninklijke Philips Electronics NV: The Netherlands.

(19) XRD reference no. 22−1086. *Natl. Bur. Stand., Monogr. (U. S.)* **1971**, *25*, 9, 22.

(20) Guilinger, J. World Industrial Minerals. Private communication, 2004.

(21) Choung, J. W.; Xu, Z.; Finch, J. A. Advances in the ambient temperature ferrite process applied to acid mine drainage treatment. *Environ. Technol.* **1999** *21*, 201−207.

(22) American Public Health Association. *Standard Methods for the Examination of Water and Wastewater*, 20th ed.; APHA: Washington, DC, 1998.

Received for review March 15, 2005. Revised manuscript received July 20, 2005. Accepted July 21, 2005.

ES050498A